Standard Issue – Article

Journal of Agricultural Engineering

https://www.agroengineering.org/

Hydraulic performance assessment on dynamic fluidic and complete fluidic sprinklers under indoor and outdoor conditions

Xingye Zhu, Jing Konng, Alexander Fordjour, Joseph Kwame Lewballah, Frank Agyen Dwomoh, Samuel Anim Ofosu, Junping Liu

Please cite this article as doi: 10.4081/jae.2024.1580

Submitted: 05/01/2023
Accepted: 27/10/202

Hydraulic performance assessment on dynamic fluidic and complete fluidic sprinklers under indoor and outdoor conditions

Xingye Zhu,[1] Jing Konng,[1] Alexander Fordjour,[2] Joseph Kwame Lewballah,[1,3] Frank Agyen Dwomoh,[2] Samuel Anim Ofosu,[2] Junping Liu[1]

[1]Research Centre of Fluid Machinery Engineering and Technology, Jiangsu University, Zhenjiang, China; [2]Department of Civil Engineering, Koforidua Technical University, Koforidua, Eastern Region, Ghana; [3]Department of Mechanical Engineering, Kumasi Technical University, Kumasi, Ashanti Region, Ghana

Correspondence: Xingye Zhu, Research Center of Fluid Machinery Engineering and Technology Jiangsu University, 301 Xuefu Road, Zhenjiang Jiangsu 212013, China.
Tel.: +86.051188780284.
E-mail: wfn_group@126.com

Key words: dynamic fluidic sprinkler; droplet size; uniformity coefficient; complete fluidic sprinkler; sprinkler irrigation.

Acknowledgments: the authors are greatly indebted to the Key R&D Project of Jiangsu Province (Modern Agriculture) (No. BE2021341), a project funded by the priority academic program development of Jiangsu University higher education institutions (No. PAPD-2018-87), and Project of Faculty of Agricultural Equipment of Jiangsu University (No. NZXB20210101).

Conflict of interest: the authors declare no potential conflict of interest.

Abstract

Since Complete Fluidic Sprinklers (CFS) cannot function well in low-pressure environments, Dynamic Fluidic Sprinkler (DFS) were developed to address this issue. In 2021, research in the field and laboratory were conducted to examine how well DFS and CFS performed hydraulically in both indoor and outdoor conditions. In this investigation, a Thiess Clima laser precipitation monitor was used to evaluate the droplet size and velocity distribution of two different types of sprinklers indoors. From the findings, DFS velocities ranged from 0.1 to 4 m/s whereas CFS ranged from 0.1 to 5.3 m/s. The maximum frequency value was obtained at velocities of 1 m/s for each combination. The DFS had a slightly greater discharge coefficient and spray pattern than the CFS. The DFS's maximum spray range was 12.2 m, while the CFS's maximum spray range was 10.8 m, with standard deviations of 1.07 and 1.66, respectively. Under high wind speed conditions, the maximum combined Coefficient of Uniformity (CU) of DFS and CFS were 81.1% and 78%, respectively. For a given pressure and sprinkler spacing, DFS delivered higher CU values than CFS, especially while running at low pressure, demonstrating that DFS offered a more favoured water distribution pattern at low pressure. At different distances from the sprinkler, the highest application rates for DFS and CFS were 6.7 mm h^{-1} at 7 m and 6.5 mm h^{-1} at 7 m, respectively. A comparison of DFS and CFS under hydraulic performance indicated that DFS had a better performance than CFS. The study can serve as a guide for how to conserve water in sprinkler-irrigated fields.

Introduction

Based on the sprinkler head or lateral movement designs, different sprinkler irrigation systems can be divided into solid-set, hand move, side roll, a big gun that is moved by line coil rotation or sprinkler vehicle, linear move, and center pivot (Keller et al. 1990; Khalil et al. 2002; Khatri et al. 2016). Sprinkler irrigation technology can help farmers adapt to climate change while also boosting agricultural productivity by using water resources more effectively (King et al. 2006). The lack of effective irrigation techniques causes irrigation water to be wasted or used excessively in the majority of the world. According to studies, many irrigation systems are ineffective, with an average of less than half of the irrigated water actually reaching the crop (Liang et al. 2016). The amount of irrigation water needed to refill the crop root zone can be applied nearly uniformly at the rate necessary to meet crop water requirements with careful consideration of nozzle diameters, operating pressure, and sprinkler spacing. As a result, installing sprinkler irrigation systems can help with water, time, and cost-effectiveness. Uniformity is a crucial factor in assessing the effectiveness of sprinkler irrigation systems (Lima et al. 2002). It is impacted by elements like the type of sprinkler and nozzle, spacing, and arrangement, weather, soil, and crop information (Liu et

al. 2007). Different combinations of these elements result in different water distribution patterns. For instance, the smallest amount of wind can cause evaporation losses by altering the droplet's direction. To achieve the most equal water application possible, an irrigation system is planned and operated. The impacts of wind, evaporation, and impact on the soil surface are determined by the droplet size distribution, according to (Edling et al. 1985; Solomon et al. 1987; Chan and Wallander, 1985 Solomon et al., 1985). For the purpose of comparing products, assessing the design, and forecasting operational circumstances (such as pressure), manufacturers are interested in understanding the size, proportion, and volume of droplets as well as where they are kept (Solomon et al., 1985). The smaller droplets created by this breakdown will decelerate quickly due to the effect of air resistance, tend to diminish the radius of the upward circulation, and as they descend, the wind will blow them back toward the sprinkler. A slight reduction in the cross-wind range is also brought on by the same type of interaction. Since low-pressure sprinkler irrigation is becoming more popular worldwide and irrigation resource efficiency and sustainability have received more attention, it is critical that high-pressure sprinkler irrigation be replaced immediately. The improvement of industrial informatization, intelligence, and networking, as well as energy-saving and environmentally friendly technologies and goods, are the unavoidable trends to actualize the modernization of agricultural production and construction (Li, et al., 2020; Liu, et al., 2022; Li, et al., 2021). Various theoretical, computational, and experimental investigations have been conducted over time to enhance the structure and hydraulic performance of Complete fluidic sprinklers (Hu et al. 2019; Dwomoh et al. 2013; Liu et al. 2018; Zhu et al. 2015; Liu et al., 2017). Their research revealed that the performance of Complete fluidic sprinkler (CFS), particularly when operating under low-pressure conditions, is severely hampered by rotational instability. In order to address the aforementioned problems, Jiangsu University's Research Center of Fluid Machinery Engineering and Technology developed the Dynamic Fluidic Sprinkler (DFS) head. The purpose of employing these two sprinkler heads was to evaluate the hydraulic performance and performance quality of the newly designed dynamic sprinkler. The objective of this study was to analyze the hydraulic performance of DFS and CFS under both indoor and outdoor conditions (Liu et al. 2022).

Materials and Methods

Structure and working principle

For this study, two types of sprinklers—the dynamic fluidic sprinkler (DFS) and the complete fluidic sprinkler (CFS)—were used with various nozzle size combinations, as shown in (Figure.1). The CFS was manufactured by Shanghai Watex Water-economizer Technology Co, Ltd., China (Li et al. 2007; Li et al. 2016; Zhu et al. 2018) and the DFS was self-developed as an experimental

sample. The working theory of (DFS) and (CFS) is based on the theory of the Coanda effect (Coanda 1936).

Experimental procedures

The study on hydraulic performance was carried out under indoor and outdoor conditions. The indoor experiment was performed at the Sprinkler Irrigation Laboratory of Jiangsu University (Jiangsu Province, China). The laboratory is circular in shape with a diameter of 44m and a height of 18m. The sprinkler heads were mounted on a 1.5m riser at a 90º angle to the horizontal. A centrifugal pump was used to supply water from a constant-level reservoir. Catch cans used in performing the experiments were cylindrical in shape, 200mm in diameter and 600 mm in height. The duration of each test lasted for an hour and the working pressure varied from 150 ~250 kPa. Water collected in each can was directly measured from the graduated cylinder. The application rate was calculated based on the depth of water in each catch can. Drop sizes and velocities were measured using a Thies Clima Laser Precipitation Monitor (LPM) from Adolf Thies GMBH and Co. KG, Gottingen, Germany. The measurement of LPM is range from 0.125 mm to 8.0 mm. Droplet size measurements were divided into 0.1 mm increments (+0.05 mm) for analysis, which lasted from 0.25 mm to 7.95 mm. Measured drops less than 0.2 mm in diameter were discarded because they account for less than 0.01% of the total volume of the measured drops. The field study was conducted at the Fisheries and Aquaculture Technology Teaching and Research Farm in Volta Region. This site was chosen for easy accessibility and availability of facilities. The Research farm is located at the latitude 7°17'N and longitude 5°14'E within the humid region of Ghana and lies in the rainforest zone with a mean annual rainfall of between 1300 and 270mm and an average temperature the relative humidity range between 85% to 100% the rainy season and less than 60% during the dry season. Water application experiments were performed under normal field conditions. The test periods were chosen such that several field tests could be performed under different wind speed conditions in order to characterize operations at different wind speeds and pressure conditions. Before and during the experiment, the surrounding weather conditions such as relative humidity, air temperature, wind speed and directions were recorded at 10 minutes intervals as each experiment lasted for one hour. The weather conditions were measured with a multipurpose handheld weather station (Smart Sensor Intellisafe) at 20m away from the testing location. For purposes of classification and easy description, the experiments performed were categorized into three wind speed groups with reference to Tarjuelo et al. (1999) as follows: low U< 1.5 m/s; moderate U<3.5 m/s; high U >3.5 m/s.

Equation (3) determines the water application rate using the Christiansen coefficient of uniformity (CU). To simulate sprinkler uniformities under varied operating pressures, Matlab software was employed. Cubic spline interpolation was used to analyze the water distribution data from a single nozzle, and the observed data was then transformed into grid format. The optimum combined water distribution maps were then generated by utilizing the superposition approach to calculate the combined uniformity coefficients for the overlapped sprinklers. The combination spacing value ranged from R to 1.8R to prevent the phenomenon of missed spraying. The parameters of centrality and droplet size dispersion were determined by the statistical analysis of the droplet data set. Average volume diameter (Dv, mm) and arithmetic mean diameter (d, mm), two droplet size characteristics employed in this work, were computed using equations (1) and (2), respectively. Equation (4) was used to calculate each nozzle's discharge coefficients based on the pressure-discharge data that had been observed.

$$\bar{d} = \frac{\sum_{i=1}^{n} m_i d_i}{\sum_{i=1}^{n} m_i} \quad (1)$$

$$d_v = \frac{\sum_{n}^{n} - = 1 d_i^{\,4}}{\sum_{n}^{n} = 1 d_i^{\,3}} \quad (2)$$

$$CU = 100\left(1 - \frac{\sum_{i=1}^{n} |X_i - \mu|}{\sum_{i=1}^{n} X_i}\right) \quad (3)$$

$$C = \frac{Q}{A\sqrt{2gH}} \quad (4)$$

Where Q is the volumetric discharge of the sprinkler ($m^3\ s^{-1}$), A is the nominal cross-sectional area of the nozzle (m^2), g is the gravitational acceleration ($m\ s^{-2}$), H is the pressure head (m), c is the discharge coefficient, and the discharge exponent for the sprinklers was 0.5.

Results and Discussion

Table 1 lists the atmospheric temperature, average wind speed (m/s), and relative humidity (0/0) that prevailed during the field test. They were typical of the weather conditions at the test site. Within the operating pressure range of 150 to 250 kPa, the recorded sprinkler flow rates ranged from 3.12 to 3.62 m^3/hr, with an average of 3.37 m^3/hr.

Comparison of discharge and spray range

Table 2 presents the summary of the discharge coefficient for both sprinkler heads. The coefficient of discharge for (CFS) ranged from 0.72~0.92 with an average value of 0.85, while that

from (DFS) was from 0.74~0.93 with an average of 0.86. The discharge coefficients for both sprinklers changed slightly when the working pressure was increased. However, the discharge coefficient of (DFS) was higher than the (CFS). The comparison of the radius of throw for the two sprinklers under the same working condition demonstrated that DFS gave a higher distance of throw. It was observed that as pressure increased the distance of throw also increased for both sprinkler heads. The maximum spray range from the DFS was 12.2 m, whiles CFS was 10.8 m and the standard deviation was 1.07 and 1.66, respectively. It was found that the spray ranges from the CFS were smaller and this could be attributed to the degree of interruption causing a small reduction in the distance travelled by the water jet.

Relationship between rotation speed for CFS and DFS heads

Figure 3 shows the quadrant completion times for both sprinkler heads at various operating pressures. Increasing pressure typically led to a decrease in rotational speed for both sprinkler heads. It was discovered that the CFS completion time varies significantly across the entire quadrant. This is in line with what Zhu et al. (2015) and Dwomoh et al. (2014).

As can be seen in (Figure.3b), the differences in quadrant completion times were 20, 18.8, 17.9, and 18 s for Q1, Q2, Q3, and Q4, respectively. The discrepancies in quadrant completion times were found to be significant, particularly at 150 kPa; this indicates that the CFS sprinkler performed poorly under low-pressure situations. This event is caused by the CFS sprinkler's stepwise rotation, which explains how the fluidic element's quick wall attachment concept works. These findings are similar with those made by (Zhu et al, 2012; Li et al, 2016). The differences in quadrant completion times at various pressures demonstrated that DFS was slower than CFS, particularly in low-pressure situations. It was found in (Figure.2a), the differences in quadrant completion times were 21, 20.6, 19.9, and 20.3 s for Q1, Q2, Q3, and Q4, respectively. The relatively regular pressure variations could be the cause. The findings of the quadrant completion times demonstrated that, as compared to CFS, DFS produced the best rotation stability under low-pressure situations.

Comparison of water distribution

Figure 4 shows the radial water distribution characteristics for the DFS and CFS sprinklers at 150, 200, and 250 kPa working pressures. The water distribution appears to be considerably higher and nearly the same for both sprinkler heads in the figures. However, even at a pressure of 150 kPa, the water distributions from the DFS sprinkler were uniform. The highest values of water distributions at the end of the spray range for the DFS sprinkler were 2.91 to 6.8 mm h^{-1}. The

maximum value of the application rate recorded for the three evaluated pressures was (6.1 mm h^{-1} at 10 m for 150 kPa, 6.23 mm h^{-1} at 7 m for 200 kPa and 6.53 mm h^{-1} at 7 m for 250 kPa,).

The maximum value of application rate recorded for the three evaluated pressures was (6.3 mm h^{-1} at 7 m for 150 kPa, 6.7 mm h^{-1} at 7 m for 200 kPa, and 6.7 mm h^{-1} at 5 m for 250 kPa). Typically, at higher operating pressures, water application intensities were smaller and more uniformly distributed. The application rate decreased abruptly as the distance increased from the source. The water distribution results that were obtained agreed with earlier studies by (Li et al. 2018; Xu et al. 2018; Lorenzini et al. 2005). The DFS sprinkler provided a higher water distribution than the CFS sprinkler when the water distribution from the two types of spray heads was compared under identical conditions. This might be related to the fluidic sprinkle's design elements. The comparison of water application rates showed that the shapes formed by DFS and CFS sprinklers were, rectangular and elliptical, respectively. The DFS sprinkler performed a little bit better at 150 kPa than it did at the other pressures. It was found that as operating pressure increased, the application rates increased until they reached the maximum when they started to decrease for both sprinklers.

Comparison of the computed uniformity coefficient

Figure 5 presents a comparison of the combined uniformity of the two sprinklers. Square spacing for lateral radius times of 1.0, 1.1, 1.2, 1.3, 1.4, 1.5, 1.6, 1.7, and 1.8 was chosen for each sprinkler after they were individually assessed using the coefficient. For the computation of the two sprinklers, various operating pressures, including 150, 200, and 250 kPa, were used. As the gap widened, the computed CU from both sprinklers first increased to a maximum and subsequently decreased, as seen in Figure 5. For example, the simulated DFS CU spray range increased from 75% at R to 89% at 1.6R (150 kPa), from 73% at R to 84.5% at 1.6R (200 kPa), and from 74% at R to 86% at 1.3R (250 kPa). The uniformities for the various pressures increased with spacing from 1 to 1.8R, averaging 81.2, 78.5, and 77%, respectively. The estimated CU from CFS also increased, with average uniformities of 75.6, 76.29, and 77.04%, respectively, from 69% at R to 83% at 1.6R (150 kPa), 69% at R to 84% at 1.6R (200 kPa), and 72% at R to 85% at 1.6R (250 kPa). When the coefficient of uniformity of different types was compared, it was shown that DFS had higher CU and CFS had the lowest. The findings demonstrate that DFS had greater simulated CU for all sprinkler spacings taken into account.

Droplet size distribution

Figure 6 presents droplet sizes for both sprinkler types at different operating pressures. Generally, larger droplet sizes were produced at low pressure and as pressure increased small droplet sizes were recorded for both sprinklers. From the study, it was observed that as the distance to sprinkle increases, the frequency of large drops increases. The average droplet diameter of DFS ranged from 0 to 4 mm. The average CFS droplet diameters ranged from 0 to 5.3 mm. Table 2 presents the cumulative frequencies for both sprinkler heads. A comparison of DFS and CFS curves indicate that 60% of the droplet had a diameter < 3.5mm for DFS. Within a certain distance from the sprinkler, the average droplet sizes of the two sprinklers were similar. The minimum droplet size was generated by the CFS, and the droplet size produced by the CFS is smaller than the increase rate of the minimum droplet diameter. Losses through evaporation and wind drift increased greatly as droplet size decreased from 0.6 to 0.3 mm (Molle 2002; Liu et al. 2017). However, the droplet sizes from DFS were larger because the maximum droplet diameter decreased and was larger than the increase rate of the minimum droplet size diameter. It means that the DFS may be useful to minimize evaporation and wind drift losses while preventing damage to the soil under field conditions.

Droplet velocity distribution

The mean droplet velocities from the two sprinkler types at various operating pressures are shown in Figure 7. The following observations were made for both sprinklers: Figure shows that the mean droplet velocities from the DFS sprinkler ranged from 0.1 to 5.7 m/s. For pressures of 150, 200, and 250 kPa, the droplets at 1 m/s, 3 m/s, and 5 m/s had frequencies of 29, 24.5, and 22%, 6.7, 8, and 9%, and 5.8, 4.5, and 5.2%, respectively. Under CFS, mean velocities of 0 to 6.3 ms−1 were also attained. For pressures of 100, 150, and 200 kPa, frequencies of 25, 24, and 23.5% were seen at 1 ms−1, under 3 ms−1, 7, 8.5, and 9.1%, and under 5 ms1, of 4.8, 3.7, and 4.6%, respectively. The figure shows that the huge droplet sizes caused the velocity distribution of the droplets from the DFS sprinkler to be significantly larger. The findings demonstrated that the velocities of DFS and CFS droplets were comparable but not identical, and it was possible to see a distribution of velocities that was very close. Additionally, the operating pressure and the distance from the sprinkler to the target surfaces during spraying greatly impact droplet diameter (Hills and Gu 1989; Liu et al. 2017).

Water distribution pattern analysis

Figure 8 presents the relationship between water distribution under low, medium and high wind speed for CFS sprinkler at low. It can be observed that the wind distortion of the water

distribution pattern concentrates in particular areas of the experimental field. The CFS application intensity changed depending on the pressure (4.2 mm h^{-1} at 7 m for 150 kPa, 4.69 mm h^{-1} at 7 m for 200 kPa and 4.8mm h^{-1} at 7 m for 250 kPa, respectively). The reason for these patterns is the uneven rotation of the opposing wind, which focuses sprinklers in one location and causes minute droplets to gather at high wind speeds. As a result, the application intensity varies little, which lowers the CU value. The range of application intensity broadens as the wind blows continuously in one direction. In low wind conditions, water application intensities are lower and the distribution is more even than in high wind conditions. This relationship explains 78 % of the variation of the CU. For wind speeds beyond 2ms−1, the value of CU is clearly affected by the wind speed. These findings agree with those presented in publications by Tarjuelo et al. (1994) and Dechmi et al. (2003b).

The relationship between water distribution for DFS sprinklers operating at low, medium, and high wind speeds is shown in Figure 9. It is evident that specific regions of the experimental field are more affected by wind-driven water distribution pattern distortion. The DFS application intensity changed depending on the pressure (4.5 mm h^{-1} at 7 m for 150 kPa, 4.7 mm h^{-1} at 7 m for 200 kPa and 4.8mm h^{-1} at 7 m for 250 kPa, respectively). This seems to be due to the variability of wind speed and direction during the irrigation time. As a result, there are minimal variations in the application intensity, which lowers the Cu value. As the wind blows constantly in a single direction, the range of application intensity increases. Water application intensities are lower and the distribution is more even under low-wind situations than in high-wind ones. Wind speed clearly affects the value of CU with wind speeds greater than 2ms−1.

Relationship between wind speed and uniformity

Figure 10 and 11 present the relationship between wind speed and uniformity under low, medium and high speed for CFS and DFS. The CU values from DFS varied from 74% at R to 86% at 1.6R (150 kPa), 72% at R to 83% at 1.6R (200 kPa), and 73% at R to 85% at 1.6R (250 kPa), all of which were high at low wind speeds. Similar to this, the predicted CU from the CFS were 72% at R to 84% at 1.6R (250 kPa), 67% at R to 80% at 1.6R, and 68% at R to 82% at 1.6R, respectively, with average uniformities of 75.6, 76.29, and 77.04%. The DFS's uniformity ratings varied from 85.5% at 250 kPa operating pressure to 81.5% at moderate wind speed conditions. The DFS CU values at high wind speeds ranged from 71% at R to 79% at 1.6R (150 kPa), 65% at R to 76% at 1.6R (200 kPa), and 63% at R to 75% at 1.6R (250 kPa), all of which were extremely low. Similar to this, the estimated CU from CFS varied from 58% at R to 76% at 1.6R (150 kPa), 59% at R to 76.5% at 1.6R (200 kPa), and 60% at R to 77% at 1.6R (250 kPa), respectively, with average

uniformities of 73.6, 74.29, and 76.04%. The results show that using both sprinklers at wind speeds greater than or equal to 3.5 m/s is not recommended. It is important to note that low to moderate wind speeds had little impact on the CU values since they were nearly unchanged under both regimes. This confirms findings from other studies (Dukes, 2006; Zhu et al., 2015; Liu et al., 2018; Xu et al., 2018) that have already been established. The findings demonstrate that DFS had greater simulated CU for all sprinkler spacings taken into account. The results show that using both sprinklers at wind speeds greater than or equal to 3.5 m/s is not recommended. It is important to note that low to moderate wind speeds had little impact on the CU values since they were nearly unchanged under both regimes. This confirms findings from other studies (Dukes, 2006; Zhu et al., 2015; Liu et al., 2018; Xu et al., 2018) that have already been established. The findings demonstrate that DFS had greater simulated CUs for all sprinkler spacings taken into account.

Conclusions

The study of the hydraulic performance of DFS and CFS under both indoor and outdoor conditions was conducted. The following conclusions can be drawn from the study.

The maximal combined CU of DFS and CFS were 81.1, and 78 %, respectively under high wind conditions. DFS produced higher CU values than the CFS for a given pressure and sprinkler spacing, especially when operated at low pressure, indicating that DFS provided a more acceptable water distribution pattern at low pressure.

The results showed that CFS had a lower average application rate than the DFS under both indoor and outdoor conditions. With regard to distance from the sprinkler, the maximum values of application rate recorded for DFS and CFS were 6.7 mm h^{-1} at a distance of 7 m and 6.5 mm h^{-1} at a distance of 7m, respectively.

Velocities from the DFS sprinkler ranged between 0.1 to 4 m/s, while that from the CFS sprinkler ranged from 0.1to 5.3m/s. The maximum frequency value was obtained at velocities of 1 m/s for each combination.

The discharge coefficient and spray range of the DFS was slightly larger than that of the CFS. The maximum spray range from the DFS was 12.2 m, whiles CFS was 10.8 m and the standard deviation for both 1.07 and 1.66, respectively.

The results of the current study indicated that wind speed had significant effects on the coefficient of uniformity and application intensity.

A comparison of DFS and CFS under hydraulic performance indicated that DFS had a better performance than CFS. Further research is needed on sprinkler irrigation performance on a small-growth crop canopy and its effects on crop agronomics.

References

Chan, D. and W. W. Wallender. 1985. Droplet size distribution and water application with a low-pressure sprinkler.Trans ASAE, 11: 801-803

Chen, X. X., Wang, C., Shi, W. D., Zhang, Y. C. 2020. Numerical simulation of submerged impinging water jet at different impact angles[J]. Journal of Drainage and Irrigation Machinery Engineering, 38(7): 658-66

Coanda, H.1936. Device For Deflecting a Stream of Elastic Fluid Projected Into an Elastic Fluid. U.S. Patent No. 2,052,869

Dukes M D. 2006. Effect of wind speed and pressure on linear move irrigation system uniformity[J]. Applied Engineering in Agriculture, 22(4):541-548.

Dwomoh, F.A., Yuan, S. and H. Li. 2013. Field performance characteristics of a fluidic sprinkler. Applied Engineering in Agriculture. 29(4): 529–536.

Dwomoh, F.A., Yuan, S.and H. Li. 2014. Droplet size characterization of the new type complete Fluidic sprinkler. IOSR Journal of Mechanical and Civil Engineering, (11): 70-73.

Edling, R. J. 1985. Kinetic energy, evaporation and wind drift of droplets from low pressure irrigation nozzles. Transactions of the ASAE. (286): 1543-15500.

Hills, D. J., and Y. Gun. 1989. Sprinkler volume droplet diameter as a function of pressure. Transactions of the ASAE, (32):471-476.

Hu, G., Zhu, X. Y., Yuan, S. Q., Zhang, L. G., and Y. F Li. 2019. Comparison of ranges of fluidic sprinkler predicted with BP and RBF neural network models. J Drain Irrig Mach Eng, 37(3): 263-269.

Keller, R. D., and R. D. Bliesner. 1990. Sprinkler Irrigation. Van Nostrand Reinhold, USA, New York.

Khalil, M. F., Kassab, S .Z., and A. A. Elmiligui. 2002. Applications of drag-reducing polymers in sprinkler irrigation systems Sprinkler head performance. Journal of Irrigation and Drainage Engineering ASCE, 128(3): 147–152.

Khatri, A., Aggarval, and P. K. Joshi. 2016. Farmers' priotization of climatesmart agricultureal technologies. Agriculture systems, (151): 184–191.

King, B. A., Stark, J .C., and R. W.Wall. 2006. Comparison of site-specific and conventional uniform irrigation management for potatoes. Applied Eng in Agric, 22(5) :677– 688.

Lorenzini G. and D. Wrachien. 2005. Performance assessment of sprinkler irrigation systems: a new indicator for spray evaporation losses. Irrigation and drainage 54 (3): 295-305.

Li, H., Yuan, S. Q., Liu, J. P., Xiang, Q.J., Zhu, X. Y.,and F. Q. Xie. 2007. Wall-attachment fluidic sprinkler. Ch. Patent No. 101224444 B.

Li, H., Tang, P., Chen, C., Zhang, Z. Y., Xia, H. M. 2021. Research status and development trend of fertilization equipment used infertigation in China[J]. Journal of Drainage and Irrigation Machinery Engineering, 39(2): 200-209.

Li, Y. B., Liu, J. P. 2020. Prospects for development of water saving irrigation equipment and technology in China. Journal of Drainage and Irrigation Machinery Engineering, 38(7): 738-742.

Li, L. H., Zhang, X. Y., Qiao, X. D., and G .M. Liu. 2016. Analysis of the decrease of center pivot sprinkling system uniformity and its impact on maize yield. Int J Agric & Biol Eng, 9(4): 108－119.

Li, Y. F., Liu, J. P., Li, T., and J. E. Xu. 2018. Theoretical model and experiment on fluidic sprinkler wet radius under multi-factor. J Drain Irrig Mach Eng, 36(8): 685-689.

Liang, X. Z., Wu, Y., Chambers, G .R., Schmoldt, L. D., Gao, C., Yan, L. L., Sun, C., and A. J. Kennedy. 2016. Determining climate effects on US total agricultural productivity. National Academy of Sciences, 114(12): 2285–2292.

Lima, J .L., Torfs, P. J. F., and V. P Singhc. 2002 .A mathematical model for evaluating the effect of wind on downward-spraying rainfall simulators. Catena, 46(2002): 221–241.

Liu, J. P., Li, T., Zhang, Q. 2021. Experimental study on influence of flow channel structure on hydra-ulic performance of low-pressure rotary sprinkler[J]. Journal of Drainage and Irrigation Machinery Engineering, 39(3): 312-317.

Liu, J.P., Liu ,W.Z., Bao, Y. Zhang, Q. and X.F. Liu. 2017. Drop size distribution experiments of gas-liquid two phases fluidic sprinkler. J Drain Irrig Mach Eng, 35(8): 731-736.

Liu, H .J., and Y. H. Kang. 2007.Sprinkler irrigation scheduling of winter wheat in the North China Plain using 20 cm standard pan. Irrig Sci, (25): 149–159.

Liu, H. J., Kang, Y. H., and S .P. Liu. 2003. Regulation of field environmental condition by sprinkler irrigation and its effect on water use efficiency of winter wheat. Trans China Soc Agric Eng, 19: 46–51.

Liu, J .P. Zhu, X.Y. Yuan S .Q. and X. F. Liu. 2018. Droplet motion model and simulation of a complete fluidic sprinkler. Transactions of the ASABE, 61(4): 1297-1306.

Molle B. 2002. Characterizing droplet distribution of an irrigation sprinkler water application. In Food production, poverty alleviation and environmental challenges as influenced by limited water resources and population growth. Volume IA. 18th International Congress on Irrigation and Drainage, Montréal, Canada, 2002. 1-19.

Shi, Y. J., Zhu, X. Y., Hu, G., Zhang, A. Y., Li, J. P. 2021. Effect of water distribution on different working conditions for spri-nkler irrigation[J]. Journal of Drainage and Irrigation Machinery Engineering, 39(3): 318-324.

Solomon, K .H. 1987.Sprinkler irrigation uniformity. ASPAC, Food and Fertilizer Technology Center, Taiwan. Extension Bulletin No.247, 1987.

Xu, Z. D., Li, H., Xiang, Q. J., Wang, J. H., Jiang, Y., Liu J. 2022. Effect on combination irrigation of low pressure 20PY2 impact sprinkler with and without aeration[J]. Journal of Drainage and Irrigation Machinery Engineering, 40(1): 74-79.

Xu Z.D. Xiang Q.J, Waqar A.Q. and J. Liu 2018. Field combination experiment on impact sprinklers with aerating jet at low working pressure. J Drain Irrig Mach Eng, 36(9): 840-844.

Zhang, Q., Liu, J. P., Yuan, S. Q., Li, Y. F., Li, H. 2022. Structure design and hydraulic performance test of water and pesticide integrated sprinkler[J].Journal of Drainage and Irrigation Machinery Engineering, 40(1): 102-108.

Zhang, Z. H., Sun, X. D., Xie, J. P., Li, H., Zhang, D. J., Jiang, T. T., Lyu, M. L., Hua, L. 2022. Numerical simulation of water-sand phase flow in regulator channel of micro-sprinkler irrigation system[J].Journal of Drainage and Irrigation Machinery Engineering, 40(2): 211-216.

Zhu X.Y. Yuan S.Q. and J.P Liu. 2012. Effect of sprinkler head geometrical parameters on hydraulic Performance of fluidic sprinkler. J. *Irrig. Drain. Eng.,* 138(11): 1019-1026.

Zhu X. Yuan S. Jiang J. Liu J. and X Liu. 2015. Comparison of fluidic and impact sprinklers based on hydraulic performance. *Irrig. Sci.,* 33:367–374.

Zhu X.Y. Fordjour A. Yuan S.Q. Dwomoh F. and D.X Ye. 2018. Evaluation of hydraulic performance characteristics of a newly designed dynamic fluidic sprinkler. Water, 10, 1301; doi: 10.3390/w10101301

Zhu, X. Y., Zhang, A. Y., Zhang, L. G., Shi, Y. J., Jiang, N. 2021. Research on atomization performance of low-pressure atomization nozzle[J]. Journal of Drainage and Irrigation Machinery Engineering, 39(2): 210-216.

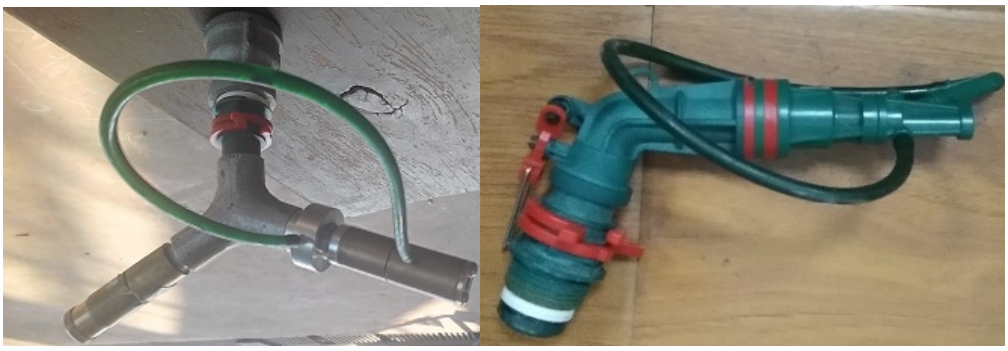

(a) dynamic fluidic sprinkler (b) complete fluidic sprinkler

Figure 1. A prototype of the dynamic fluidic and complete fluidic sprinklers.

Figure 2. Schematic diagram of the experimental apparatus.

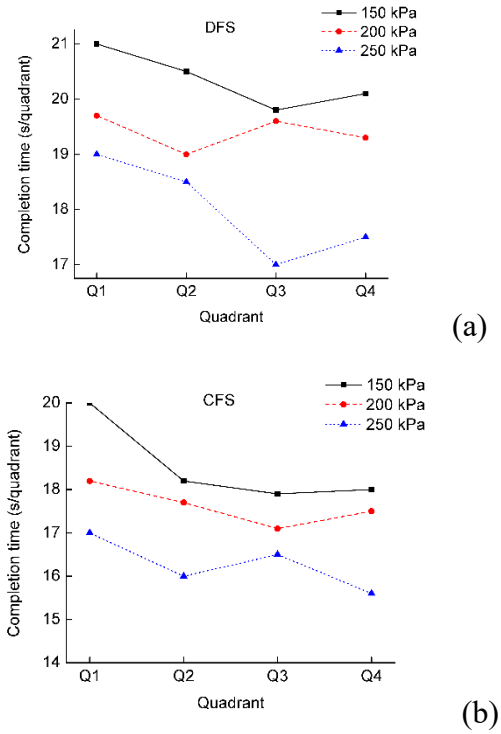

Figure 3. Quadrant completion time under different operating pressures for both sprinkler heads.

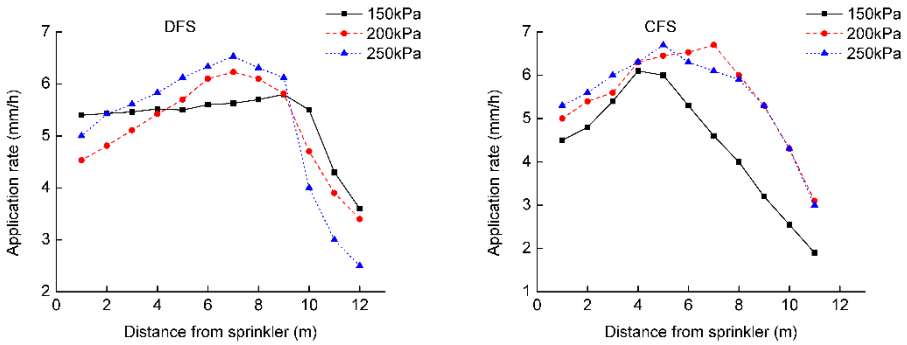

Figure 4. Radial water distributions profiles for the DFS and the CFS.

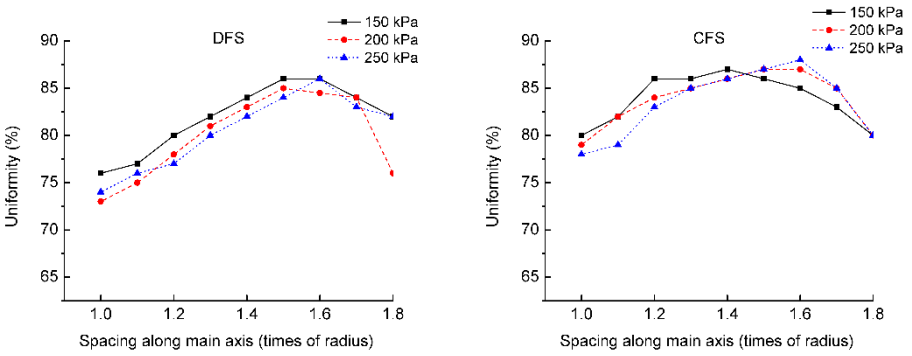

Figure 5. Comparison of the combined uniformity of the two sprinklers.

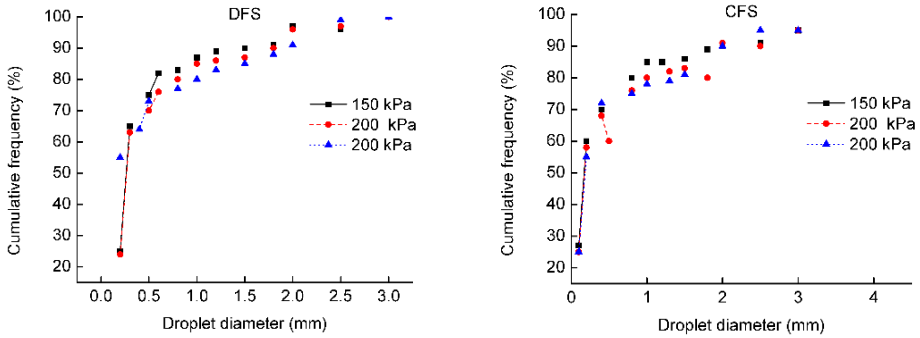

Figure 6. Droplet sizes for both sprinkler types at different operating pressures.

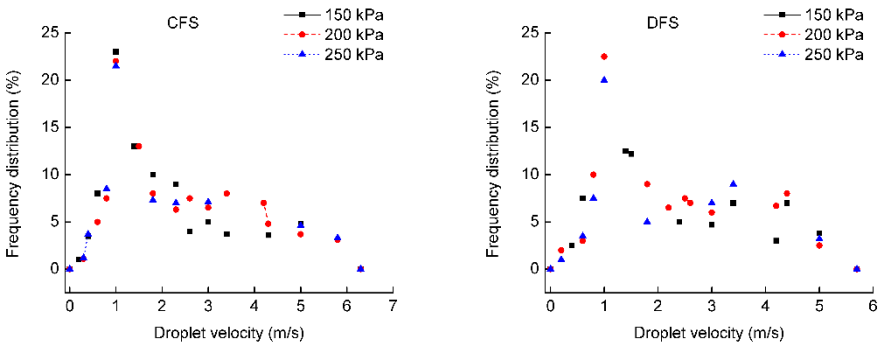

Figure 7. Relationship between frequency and droplet velocity for both sprinkler heads.

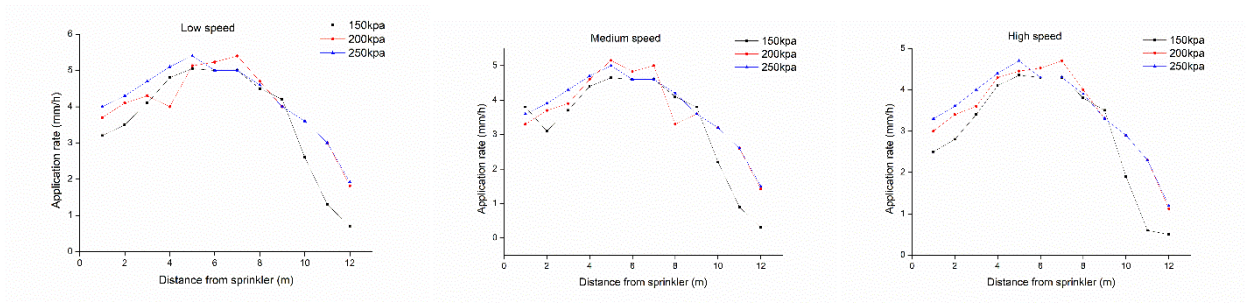

Figure 8. Relationship between water distribution under low, medium and high wind speed for (CFS).

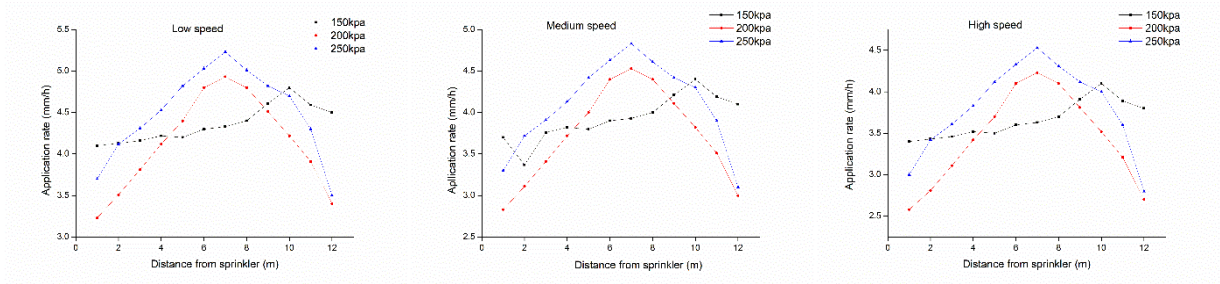

Figure 9. Relationship between water distribution under low, medium and high wind speed for (DFS).

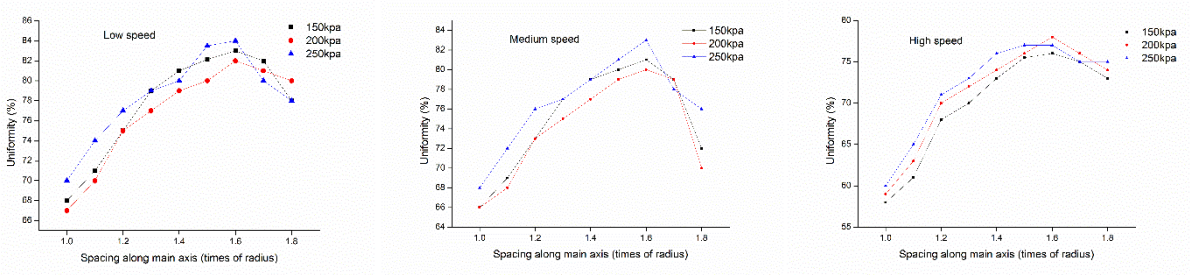

Figure 10. Relationship between wind speed and uniformity under low, medium and high for (CFS).

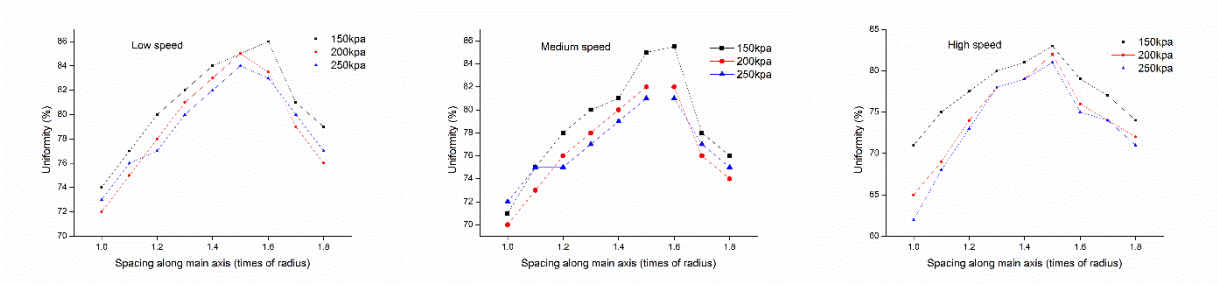

Figure 11. Relationship between wind speed and uniformity under low, medium and high for (DFS).

Table 1. The maximum, minimum and average wind speed (m/s), air temperature and relative humidity.

Parameters	Maximum	Minimum	Average
Wind Speed(m/s)	(3.5-5)	(2-3)	(0.5-1.5)
Relative Humidity (^{0}/0)	86.9	60.9	78.9
Air Temp.(^{0}C)	29.4	24.5	26.95

Table 2. Summarized discharge coefficient for both sprinkler heads.

Radius of throw (m)							Discharge coefficient				
Sprinkler type	Nozzle size (mm)	Pressure (kPa)	150	200	250	Standard deviation	Pressure (kPa)	150	200	250	Standard deviation
(CFS)	5		8.2	10.1	11.5	1.66		0.72	0.90	0.92	0.096
(DFS)	5		12.2	10.5	10.2	1.07		0.93	0.91	0.74	0.10

Table 3. Cumulative frequencies for both sprinkler heads.

Droplet diameter	Pressure/Kpa					
	150		200		250	
	Cumulative frequencies /%		Cumulative frequencies /%		Cumulative frequencies /%	
	DFS	CFS	DFS	CFS	DFS	CFS
1mm	85	84	84	84	79	79
2mm	95	90	91	91	90	89
Droplet diameter	Pressure/Kpa					
	150		200		250	
	Cumulative frequencies /%		Cumulative frequencies /%		Cumulative frequencies /%	
	DFS	CFS	DFS	CFS	DFS	CFS
3mm	97	95	98	95	94	95
4mm	100	97	100	98	100	96